Electronic band structures of Ge1−xSnx semiconductors: A first-principles density functional theory study

Ming-Hsien Lee, Po-Liang Liu, Yung-An Hong, Yen-Ting Chou, Jia-Yang Hong et al.

Citation: J. Appl. Phys. **113**, 063517 (2013); doi: 10.1063/1.4790362
View online: http://dx.doi.org/10.1063/1.4790362
View Table of Contents: http://jap.aip.org/resource/1/JAPIAU/v113/i6
Published by the American Institute of Physics.

JOURNAL OF APPLIED PHYSICS **113**, 063517 (2013)

Electronic band structures of $Ge_{1-x}Sn_x$ semiconductors: A first-principles density functional theory study

Ming-Hsien Lee,[1] Po-Liang Liu,[2,a)] Yung-An Hong,[2] Yen-Ting Chou,[2] Jia-Yang Hong,[2] and Yu-Jin Siao[2]
[1]*Department of Physics, Tamkang University, Tamsui, Taipei, Taiwan 251*
[2]*Graduate Institute of Precision Engineering, National Chung Hsing University, Taichung, Taiwan 402*

(Received 17 September 2012; accepted 21 January 2013; published online 13 February 2013)

We conduct first-principles total-energy density functional calculations to study the band structures in $Ge_{1-x}Sn_x$ infrared semiconductor alloys. The norm-conserving optimized pseudopotentials of Ge and Sn have been constructed for electronic structure calculations. The composition-bandgap relationships in $Ge_{1-x}Sn_x$ lattices are evaluated by a detailed comparison of structural models and their electronic band structures. The critical Sn composition related to the transition from indirect- to direct-gap in $Ge_{1-x}Sn_x$ alloys is estimated to be as low as $x \sim 0.016$ determined from the parametric fit. Our results show that the crossover Sn concentration occurs at a lower critical Sn concentration than the values predicted from the absorption measurements. However, early results indicate that the reliability of the critical Sn concentration from such measurements is hard to establish, since the indirect gap absorption is much weaker than the direct gap absorption. We find that the direct band gap decreases exponentially with the Sn composition over the range $0 < x < 0.375$ and the alloys become metallic for $x > 0.375$, in very good agreement with the theoretical observed behavior [D. W. Jenkins and J. D. Dow, Phys. Rev. B **36**, 7994, 1987]. For homonuclear and heteronuclear complexes of $Ge_{1-x}Sn_x$ alloys, the indirect band gap at *L*-pointis is found to decrease homonuclear Ge-Ge bonds or increase homonuclear Sn-Sn bonds as a result of the reduced *L* valley. All findings agree with previously reported experimental and theoretical results. The analysis suggests that the top of valence band exhibits the localization of bond charge and the bottom of the conduction band is composed of the Ge 4*s*4*p* and/or Sn 5*s*5*p* atomic orbits. © *2013 American Institute of Physics*. [http://dx.doi.org/10.1063/1.4790362]

I. INTRODUCTION

The group IV semiconductors open up new doors in the development of important devices across a variety of applications such as infrared (IR) photodetectors, sensors, emitters, and related photonics systems. The radiative recombination and light absorption in semiconductor devices rely on materials possessing direct band gaps. Interestingly, none of the column IV materials are direct-gap semiconductors, such as the indirect band gap of the germanium and the zero-gap of the cubic α-tin.[1,2] Fortunately, $Ge_{1-x}Sn_x$ alloys have been wildly reported to undergo a transition from indirect- to direct-gap semiconductors for $x = 0.09$ ~0.26.[3–8] For example, Pérez Ladrón de Guevara *et al*. showed that the crossover Sn concentration from the indirect to the direct band gap in $Ge_{1-x}Sn_x$ alloys is close to the predicted value $x = 0.09$ based on observations obtained by the fast-Fourier-transform infrared interferometer (FFT-IR).[3] Using spectroscopic ellipsometry and photoreflectance, D'Costa *et al*. observed that the critical Sn composition x for a transition from the indirect to the direct band gap should be less than 0.11, since the indirect gap absorption is much weaker than the direct gap absorption and is hard to measure the critical value where the transition happens.[4] The composition-bandgap relationship in $Ge_{1-x}Sn_x$ alloys has increased the interest in using *ab initio* pseudopotential calculations in the virtual crystal approximation (VCA), but the VCA shows significant departures of experimental band gaps with increasing Sn concentrations.[3,7,8] On the other hand, Moontragoon *et al*. reported that the $Ge_{1-x}Sn_x$ band gap becomes a direct gap material for Sn content > 17% using the charge self-consistent pseudopotential $X\alpha$ calculations within a mixed-atom approximation.[9] However, the critical Sn composition (17%) related to the dominant direct-band-gap transitions, which severely overestimates the one in Ref. 3 ($0.10 < x < 0.13$), does not provide much improvement as derived by averaging over all possibilities of several random configurations at each composition of $Ge_{1-x}Sn_x$. Furthermore, first-principles calculations using the zincblende (ZB) structure were widely and theoretically evaluated to illustrate the composition-bandgap relationships of homogeneous $Ge_{1-x}Sn_x$ alloys.[10–12] For example, the electronic band structures of the ZB phase of the ordered $Ge_{0.5}Sn_{0.5}$ ($x = 0.5$) exhibit a direct small band gap (0.1 eV) investigated using a linear combination of atomic orbitals (LCAO) approach within the generalized gradient approximation (GGA) for exchange and correlation.[10] From a theoretical point of view, the screened-exchange local density approximation (sX-LDA) formalism of the exchange-correlation potential term provides very good band gaps for common IV-IV semiconductors to overcome the short-coming of standard density functional theory (DFT) methods based on GGA or LDA.[13] So far, to our knowledge, no one has predicted the composition-bandgap relationship in $Ge_{1-x}Sn_x$ lattices under the computationally much more demanding sX-LDA formalism.

a)Author to whom correspondence should be addressed. Electronic mail: liupo@ms5.hinet.net.

Synthesis of $Ge_{1-x}Sn_x$ alloys are compositional metastability due to a lower Sn surface free energy than Ge, which in turn cause surface segregation and compositional fluctuations of β-Sn defects, i.e., Sn-atoms occupying the center of Ge-divacancies with a local change of symmetry or namely the *split-vacancy* and *full-vacancy* configuration of Sn in Ge, appearing increases at larger temperatures.[14–16] In particular, the inhomogeneities were related to the appearance of non-substitutional Sn in the $Ge_{1-x}Sn_x$ alloy at higher Sn-concentrations. In contrast, homogeneous $Ge_{1-x}Sn_x$ alloys at high Sn-concentrations, Sn atoms on the substitutional site only, have been demonstrated by using nonequilibrium growth methods such as low energy molecular beam epitaxy (MBE) or low-temperature chemical vapor deposition (CVD). He *et al.* reported that the excellent crystallinity of homogeneous metastable $Ge_{1-x}Sn_x$ alloy films with Sn compositions up to $x = 0.34$ on Ge/Si(001) substrates has proved to inhibit Sn segregation without interrupting epitaxy by using ion-assisted MBE and reducing the growth temperature.[17] Moreover, the other experimental evidence showed that $Ge_{1-x}Sn_x$ alloy films as homogeneous alloys certainly for $x > 0.90$ exhibit the growth and stability of epitaxially $Ge_{1-x}Sn_x$ alloys grown on InSb and InSb/GaAs reported by Fitzgerald *et al.*[18] However, no measurements of the band gaps have been made for cubic homogeneous $Ge_{1-x}Sn_x$ alloy films above a Sn-concentration of around 20% and thus little is known about the change in electronic structure with the alloy composition which restricts their usefulness for device applications.

In this report, we model 8-atom cubic unit cells of the $Ge_{1-x}Sn_x$ alloys, in which Sn and Ge are distributed on the various substitutional sites to form alloy structures as homogeneous alloys. Second, we calculate the fully relaxed lattices of the various possible $Ge_{1-x}Sn_x$ alloys to yield the lowest energy configuration by conducting first-principles DFT sX-LDA calculations. Third, we calculate the electronic band structures of energetically favorable $Ge_{1-x}Sn_x$ alloys to predict the indirect- or direct-gap in $Ge_{1-x}Sn_x$ alloys. Finally, key theoretical findings related to structural and electronic properties are elucidated.

II. COMPUTATIONAL METHODS

To generate reliable pseudopotentials of Ge and Sn for the purpose of this study, we used the norm-conserving optimized pseudopotential generation scheme[19] implemented in opium code,[20] with the choice of q_c in the style suggested by Lee *et al.*[21] We used the neutral atomic configuration of Ge and Sn. To reproduce more reliable results of band structures and lattice constants of pure Ge and Sn, we included unbound $4d$ states as d-channel for Ge and treated $4d$ shallow core states as valence in Sn. The pseudization radii $r_c(s,p,d)$ chosen for Ge and Sn are (2.0, 2.0, 2.4) a_0 and (1.80, 2.20, 2.75) a_0, respectively. As for the wave vector cut-off, $q_c = 4.5\ a_0^{-1}$ is set for Ge and $q_c = 5.0\ a_0^{-1}$ is set for Sn. Four Bessel functions terms for the pseudo-orbitals in the core region were used for expanding pseudized wave functions and s-channels are chosen as local components in both pseudopotentials.

The structural properties and band gaps of the diamond-like cubic germanium and tin were carried out using the Cambridge serial total energy package (CASTEP).[22,23] These calculations were achieved via sX-LDA formalism in conjunction with a $4 \times 4 \times 4$ Monkhorst-Pack grid in the first Brillouin zone and a 350 eV energy cutoff. The cell dimensions and atomic positions were optimized to yield the ground state crystalline structures. Our calculated equilibrium lattice constants are 5.766 Å for germanium and 6.656 Å for α-Sn, which are consistent with previously reported experimental data ($a_{Ge} = 5.658$ Å and $a_{Sn} = 6.493$ Å) and theoretical results ($a_{Ge} = 5.625$ Å and $a_{Sn} = 6.454$ Å).[24]

The electronic band structures of various $Ge_{1-x}Sn_x$ models can be determined by the relative positions of the minimum conduction band at the Γ-, X-, and L-points in the first Brillouin zone. The Γ-point is the center of the zone. The X-points at $(2\pi/a)(1,0,0)$ are the intersections with the zone surface along the six equivalent ⟨100⟩ directions. Similarly the L-points at $(\pi/a)(1,1,1)$ are the intersections with the zone surface along the eight equivalent ⟨111⟩ directions, where a is the lattice constant. Band structures for the germanium and cubic α-tin are shown in Fig. 1, which indicate an L-point indirect band gap of 0.692 eV in Ge and a zero-gap of the cubic α-tin. The calculated band gap of Ge is consistent with the well-known values of 0.66 eV.[7,25–27]

III. STRUCTURAL PROPERTIES OF GERMANIUM-TIN ALLOYS

We undertook a series of eight-atom cubic lattice unit cells of $Ge_{1-x}Sn_x$ alloys with a Sn/Ge ratio of 1/7, 2/6, 3/5, 4/4, 5/3, 6/2, and 7/1 (where discrete Sn compositions of 12.5%, 25%, 37.5%, 50%, 62.5%, 75%, and 87.5% or $x = 0.125$, 0.25, 0.375, 0.5, 0.625, 0.75, and 0.875). The structural properties of thirteen $Ge_{1-x}Sn_x$ arrangements were modeled by randomly distributing Ge and Sn atoms within an 8-atom cubic lattice unit cell. Specifically, the $Ge_{1-x}Sn_x$ alloys of the intermediate compositions include one type each of $x = 0.125$ and $x = 0.875$ alloys, two types each of $x = 0.25$, $x = 0.375$, $x = 0.625$, and $x = 0.75$ alloys, and three types each of $x = 0.5$ alloys. The cohesive energies and equilibrium lattice constants were deduced from the resulting energy-volume data. Seven lowest energy $Ge_{1-x}Sn_x$ arrangements of the intermediate compositions are selected and denoted by $Ge_{0.125}Sn_{0.875}$, $Ge_{0.25}Sn_{0.75}$, $Ge_{0.375}Sn_{0.625}$, $Ge_{0.5}Sn_{0.5}$, $Ge_{0.625}Sn_{0.375}$, $Ge_{0.75}Sn_{0.25}$, and $Ge_{0.875}Sn_{0.125}$ models, which are isotropic arrangements. Fig. 2 shows

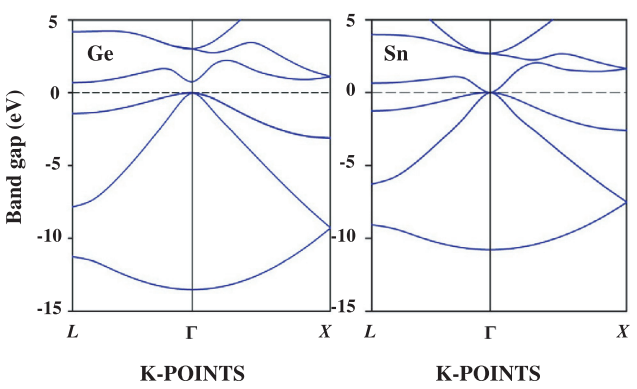

FIG. 1. Band structures of Ge and Sn. The dashed line is the Fermi level.

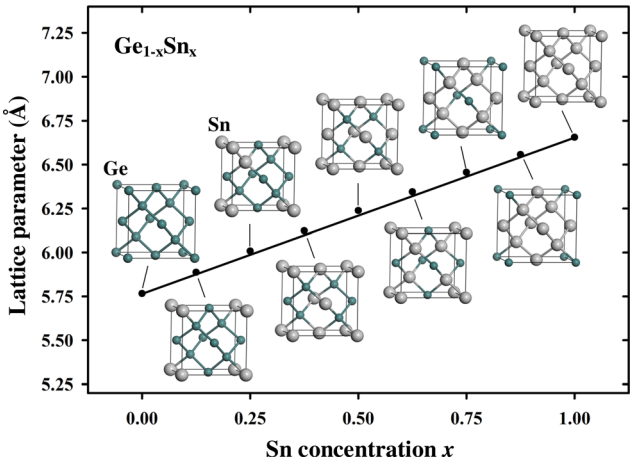

FIG. 2. Compositional dependence of lattice parameters in $Ge_{1-x}Sn_x$ alloys. The atoms are represented by spheres: Ge (green, small) and Sn (gray, large).

lattice parameters related to the pure germanium, seven isotropic $Ge_{1-x}Sn_x$ arrangements of the intermediate compositions, and α-Sn. The strong linear relation between lattice parameters and composition of $Ge_{1-x}Sn_x$ alloys exhibits Vegard behavior and can be written as $a_{Ge_{1-x}Sn_x} = a_{Sn}x + a_{Ge}(1-x) + bx(1-x)$, yielding a bowing coefficient $b = 0.104$ Å. The calculated bowing coefficient ($b = 0.104$ Å) is consistent with the reported experimental observation ($b = 0.166$ Å).[24]

IV. BAND STRUCTURES OF GERMANIUM-TIN ALLOYS

The minimum band gaps of the pure germanium, the isotropic $Ge_{1-x}Sn_x$ arrangements, and α-Sn for Γ, *X*, and *L* valleys are calculated as a function of Sn compositions described in Fig. 3. The Γ-point band gaps are exponentially dependent on Sn compositions, which showed that an exponential decay function fits the results of the Γ-point band gaps with a very high correlation coefficient of 0.9997. The dependence of the *X*-point band gap on Sn compositions exhibits a simplest linear function relation with a correlation coefficient of 0.8104. In contrast, the *L*-point band gaps are highly sensitive to Sn compositions. It is noted that Ge is characterized by an *L*-point indirect fundamental energy gap. It is apparent that isotropic $Ge_{1-x}Sn_x$ arrangements of the intermediate compositions are direct-gap semiconductors with Sn compositions in the range of $0 < x < 0.375$ and are predicted to have zero gap for $x > 0.375$, in reasonable agreement with the theoretical observed behavior.[2] The calculated indirect-direct band gap crossover in $Ge_{1-x}Sn_x$ alloys is found close to approximately tin content as low as 0.016, which is extracted from appropriate curve-fitting of Γ and *L* valley band gaps. According to previously reported theoretical results, the number of homonuclear Sn-Sn and Ge-Ge bonds or heteronuclear analogues such as Sn-Ge and Ge-Sn can change the band structure dramatically.[28] For example, for a given composition such as $Ge_{0.5}Sn_{0.5}$, one can create different pseudo-random alloys which contain various number of Ge-Ge, Sn-Sn, and Ge-Sn (or Sn-Ge) bonds, which can alter the band gap. Table I lists the results of our bonding analyses for 9 models in Fig. 2, indicating that *L*-point band gaps will be large for pure homonuclear or heteronuclear systems such as the pure germanium (16 homonuclear Ge-Ge bonds), $Ge_{0.5}Sn_{0.5}$ (16 heteronuclear Ge-Sn bonds), and α-Sn (16 homonuclear Sn-Sn bonds) as shown in Table I. In the cases of the mixture of homonuclear and heteronuclear systems, *L*-point band gaps decrease with decreasing homonuclear Ge-Ge bonds for $Ge_{0.875}Sn_{0.125}$, $Ge_{0.75}Sn_{0.25}$, and $Ge_{0.625}Sn_{0.375}$ models or increasing homonuclear Sn-Sn bonds for $Ge_{0.375}Sn_{0.625}$, $Ge_{0.25}Sn_{0.75}$, and $Ge_{0.125}Sn_{0.875}$, models.

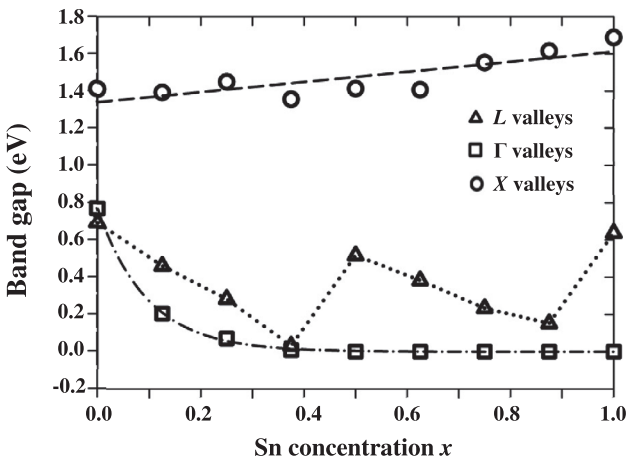

FIG. 3. Compositional dependence of band parameters at various valleys. The empty triangles, squares, and circles correspond to the *L*-point, Γ-point, and *X*-point band gaps. The top dashed line represents a linear fit to *X* valleys. The dotted line traces *L* valleys. The dashed-dotted line is an exponential fit to Γ valleys.

V. ELECTRONIC PROPERTIES OF GERMANIUM-TIN ALLOYS

The electronic property at a given alloy is obtained from DFT by analyzing the highest occupied Kohn-Sham orbitals (HOMO) and lowest unoccupied Kohn-Sham orbitals (LUMO) in conjunction with optimized atomic structures. The HOMO and LUMO isosurfaces of 9 models (see Fig. 2) are displayed in Fig. 4. We clearly see that the HOMO levels of 9 models are localized on the midpoint positions between two atoms as localized bond charge pockets (Fig. 4, left). Our 3D HOMO isosurfaces show that the homonuclear and/or heteronuclear bonds can distort the *L*-point band gaps (see Fig. 3 and Table I) but do not modify the intrinsic nature of

TABLE I. Bonding analyses of various compositions of $Ge_{1-x}Sn_x$ alloys shown in Fig. 2. Each energetically favorable $Ge_{1-x}Sn_x$ lattice has sixteen bonds dominated by three main analogues, which are referred to as the Ge-Ge, Ge-Sn, and Sn-Sn bonds.

	x								
Bond	0[a]	0.1250[b]	0.250[b]	0.375[b]	0.500[c]	0.625[c]	0.750[c]	0.875[c]	1.000[c]
Ge-Ge	16	12	9	4					
Ge-Sn		4	6	12	16	12	8	4	
Sn-Sn			1			4	8	12	16

[a]Indirect band gap
[b]Direct band gap
[c]Zero gap

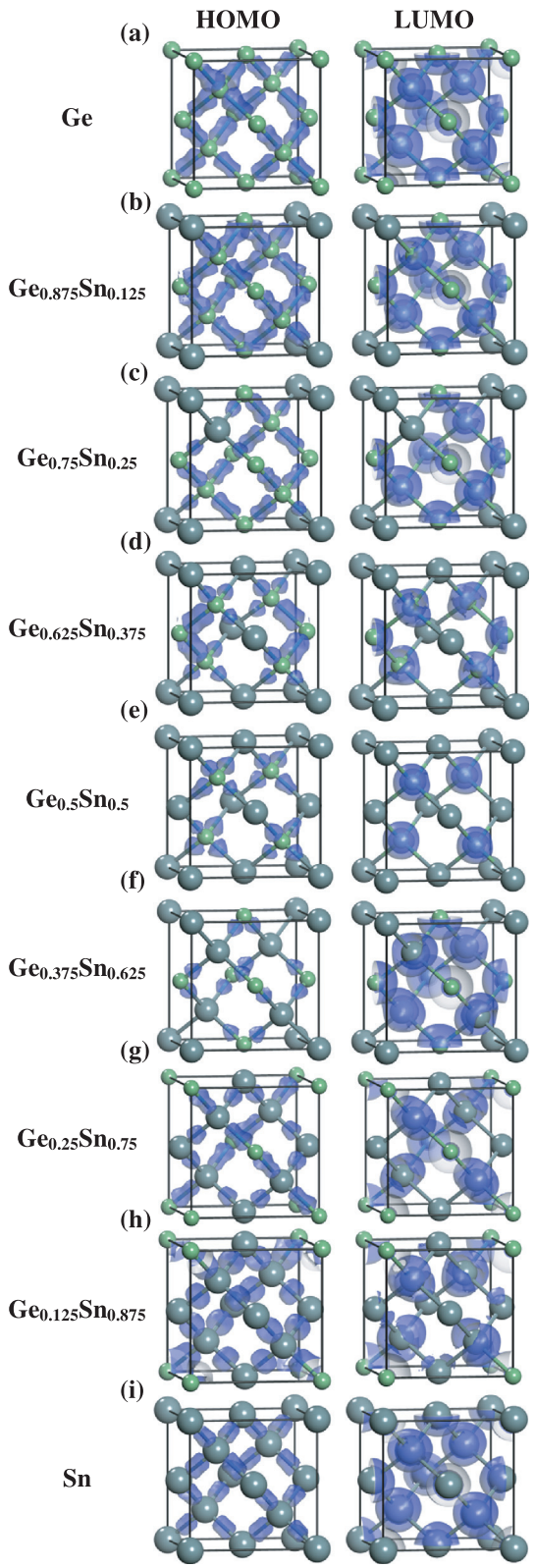

FIG. 4. HOMO and LUMO isosurfaces of $Ge_{1-x}Sn_x$ alloys denoted by the shade of blue. The atoms are represented by spheres: Ge (green, small) and Sn (gray, large).

the HOMO isosurfaces in $Ge_{1-x}Sn_x$ semiconductors. The LUMO isosurfaces are significantly different from the HOMO isosurfaces in $Ge_{1-x}Sn_x$ semiconductors (see Fig. 4). In cases of pure homonuclear systems of pure Ge and Sn, the LUMO level is solely localized in the Ge $4s4p$ or Sn $5s5p$ atomic orbits as shown in Figs. 4(a) and 4(i). For pure heteronuclear systems of $Ge_{0.5}Sn_{0.5}$ composed of 16 heteronuclear Ge-Sn bonds, the interesting feature of the LUMO is characteristic of a ubiquitous distribution of only localized Ge $4s4p$ atomic orbits as shown in Fig. 4(e). In the cases of the $Ge_{0.875}Sn_{0.125}$, $Ge_{0.75}Sn_{0.25}$, and $Ge_{0.625}Sn_{0.375}$ arrangements, the LUMO isosurfaces tend to significantly occupy orbitals around Ge atoms as shown in Figs. 4(b)–4(d). In the case of the $Ge_{0.375}Sn_{0.625}$, $Ge_{0.25}Sn_{0.75}$, and $Ge_{0.125}Sn_{0.875}$ arrangements, the LUMO levels are not only around Ge atoms but also occupied Sn atoms. Thus, the LUMO isosurfaces are composed mainly of the $4s4p$ states of the Ge and the $5s5p$ states of the Sn atomic orbits as shown in Figs. 4(f)–4(h). Our LUMO isosurfaces with Sn compositions in the range $0 \leq x \leq 0.5$ show that the spatial distribution of localized orbitals exists in the Ge $4s4p$ bands, indicating that the various configurations of Ge-Ge homonuclear and Ge-Sn heteronuclear bonds may not alter the orbital occupancy of the conduction band state in $Ge_{1-x}Sn_x$ semiconductors as observed in Figs. 4(a)–4(e). In the cases of LUMO isosurfaces with Sn compositions in the range $0.5 < x < 1$, the spatial distribution of localized orbitals exists both in the Ge $4s4p$ bands and in Sn $5s5p$ bands as seen in Figs. 4(f)–4(h), suggesting a possible explanation in a strongly effective coupling due to the increasing Sn-Sn homonuclear bonds.

VI. CONCLUSIONS

High quality band structures of $Ge_{1-x}Sn_x$ alloys were studied by first-principles total-energy density functional sX-LDA calculations. The trend of band gap variation with respect to the concentration of elements of $Ge_{1-x}Sn_x$ alloy is found computationally. Specifically, our results show that Γ-point band gaps have exponential dependence on Sn compositions and L-point band gaps decrease with decreasing the number of Ge-Ge bonds or increasing the number of Sn-Sn bonds. The calculated band gap with a composition of 0.016 tin content exhibits the change from indirect to direct band gap. Analysis of 3D contour maps for the HOMO and LUMO levels suggests that localized bond charge pockets contribute to the valence bands and the $4s4p$ states of the Ge and the $5s5p$ states of the Sn atomic orbits cover an energy range of the bottom of the conduction band.

ACKNOWLEDGMENTS

This work was supported by the National Science Council under Contract No. NSC95-2112-M-005-015-MY3, NSC99-2112-M-032-008 and in part by the Ministry of Education, Taiwan under the ATU plan. Computational studies were performed using the resources of the National Center for High-performance Computing.

[1]A. Continenza and A. J. Freeman, Phys. Rev. B. **43**, 8951 (1991).
[2]D. W. Jenkins and J. D. Dow, Phys. Rev. B **36**, 7994 (1987)
[3]H. Pérez Ladrón de Guevara Guevara, A. G. Rodrguez, H. Navarro-Contreras, and M. A. Vidal, Appl. Phys. Lett. **84**, 4532 (2004).
[4]V. R. D'Costa, C. S. Cook, A. G. Birdwell, C. L. Littler, M. Canonico, S. Zollner, J. Kouvetakis, and J. Menndez, Phys. Rev. B **73**, 125207 (2006).

[5]K. A. Mäder, A. Baldereschi, and H. V. Kanel, Solid State Commun. **69**, 1123 (1989).
[6]A. V. G. Chizmeshya, M. R. Bauer, and J. Kouvetakis, Chem. Mater. **15**, 2511 (2003).
[7]M. R. Bauer, J. Tolle, C. Bungay, A. V. G. Chizmeshya, D. J. Smith, J. Menéndez, and J. Kouvetakis, Solid State Commun. **127**, 355 (2003).
[8]G. He and H. A. Atwater, Phys. Rev. Lett. **79**, 1937 (1997).
[9]P. Moontragoon, Z. Ikonić, and P. Harrison, Semicond. Sci. Technol. **22**, 742 (2007).
[10]R. Pandey, M. Rérat, and M. Causà, Appl. Phys. Lett. **75**, 4127 (1999).
[11]W.-J. Yin, X.-G. Gong, and S.-H. Wei, Phys. Rev. B. **78**, 161203(R) (2008).
[12]M. Lv, Z. Chen, and R. Liu, Mater. Lett. **60**, 1144 (2006).
[13]B. Lee and L.-W. Wang, C. D. Spataru, and S. G. Louie, Phys. Rev. B. **76**, 245114 (2007).
[14]C. I. Ventura, J. D. Fuhr, and R. A. Barrio, Phys. Rev. B. **79**, 155202 (2009).
[15]S. Decoster, S. Cottenier, U. Wahl, J. G. Correia, and A. Vantomme, Phys. Rev. B. **81**, 155204 (2010).
[16]V. P. Markevich, A. R. Peaker, B. Hamilton, V. V. Litvinov, Y. M. Pokotilo, S. B. Lastovskii, J. Coutinho, A. Carvalho, M. J. Rayson, and P. R. Briddon, J. Appl. Phys. **109**, 083705 (2011).
[17]G. He and H. A. Atwater, Appl. Phys. Lett. **68**, 664 (1996).
[18]E. A. Fitzgerald, P. E. Freeland, M. T. Asom, W. P. Lowe, R. A. Macharrie, B. E. Weir, A. R. Kortan, F. A. Thiel, Y.-H. Xie, A. M. Sergent, S. L. Cooper, G. A. Thomas, and L. C. Kimerling, J. Electron. Mater. **20**, 489 (1991).
[19]A. M. Rappe, K. M. Rabe, K. Kaxiras, and J. D. Joannopoulos, Phys. Rev. B **41**, 1227 (1990).
[20]See http://opium.sourceforge.net/index.html for information about the Opium pseudopotential generation project.
[21]M.-H. Lee, J.-S. Lin, M.C. Payne, V. Heine, V. Milman, and S. Crampin, Ψ_k Newsletters **67** (February) Highlights (2005).
[22]M. C. Payne, M. P. Teter, D. C. Allan, T. A. Arials, and J. D. Joannopoulos, Rev. Mod. Phys. **64**, 1045 (1992).
[23]V. Milman, B. Winkler, J. A. White, C. J. Pickard, M. C. Payne, E. V. Akhmatskaya, and R. H. Nobes, Int. J. Quantum Chem. **77**, 895 (2000).
[24]P. Aella, C. Cook, J. Tolle, S. Zollner, A. V. G. Chizmeshya, and J. Kouvetakis, Appl. Phys. Lett. **84**, 888 (2004).
[25]G. Sun, R. A. Soref, and H. H. Cheng, J. Appl. Phys. **108**, 033107 (2010).
[26]J. Liu, X. Sun, D. Pan, X. Wang, L. C. Kimerling, T. L. Koch, and J. Michel, Opt. Express **15**, 11272 (2007).
[27]J. Menendez and J. Kouvetakis, Appl. Phys. Lett. **85**, 1175 (2004).
[28]J. Tolle, A. V. G. Chizmeshya, Y.-Y. Fang, J. Kouvetakis, V. R. DCosta, C.-W. Hu, J. Menndez, and I. S. T. Tsong, Appl. Phys. Lett. **89**, 231924 (2006).